

EXACT CALCULATIONS FOR ONE PHOTON MICROMASER WITH COHERENT INPUTS I

A.M. Kremid*

Physics Department, Faculty of Science, Tripoli University, Tripoli, Libya

***Corresponding Author:-**

Email: kremidzg@gmail.com

Abstract:-

We report a numerical simulation of the action of the one ^{85}Rb atom micromaser which shows that the micromaser field evolves towards a steady state equilibrium when the condition that $T_p \gg t_{int}$ satisfies. In this steady state regime the cavity field reaches a steady state after a sufficient number of atoms have passed through the cavity. The cavity temperature T and the cavity quality factor Q can produce a quantitative change when one of them or the two are changed but they are not responsible for the qualitative changes in the micromaser field. Evidently the only responsible parameter for these qualitative changes is the repetition time T_p namely if $T_p \gg t_{int}$ then the micromaser field evolution is towards a steady state equilibrium. In contrast when T_p reduced to the order of t_{int} then the micromaser field evolution is controlled by the trapping state dynamics – no steady state is apparent in this case. The first going-up trapping state at $n=3$ plays a significant role in the early dynamics of the micromaser field. Moreover the state of the field ultimately evolves towards a mixed state rather than a pure state.

Keywords:- *Micromaser, trapping states, coherent superposition.*

INTRODUCTION

The quantum theory of the micromaser was first developed by Myster et. al.[1]. This theory is a direct application of the quantum theory of the laser to a problem of two level Rydberg atoms interacting with a single mode radiation field in a microwave cavity [2-8]. In most studies of the one photon micromaser theory the injection of atoms assumes to have Poisson distribution and all atoms always entered the cavity in their excited (upper) states. This device, the micromaser, exhibits highly non-classical features such as a sub-Poisson statistics for the field, quantum revivals and trapping states. The most of these features are experimentally realized [9-11]. In this work we assume that the atoms are pumped into the cavity in a coherent superposition of their upper and lower atomic states and the cavity is at finite temperature T. Our concern is about the effects of the black body radiation in the cavity (initial thermal field) and the effects of the damping rate on the evolution of the micromaser cavity field coupled to a heat bath at temperature T. for the measurement of the EPH - International Journal of Applied Science | ISSN: 2208-2182

urity of the state reached by the cavity field we employ the entropy $S = -T_r \rho \ln \rho$. This work organized as follows: in section 2 the model and the calculations of the equations of motion are introduced while in section 3 the solution to the equations of motion is introduced. The numerical results and their discussions are given in the fourth section and at the last section the conclusion is given.

The Model

The micromaser consists of two level Rydberg atomic beam (i.e. ^{85}Rb atoms) pumped into a high-Q microwave cavity containing a single mode radiation field such that only one atom at any given time is present inside the cavity and the atom flies through the cavity in a very short time compared to the time between any two successive atoms in the atomic beam. It has been assumed that no coupling between the single mode and the heat bath during the interaction time t_{int} so when the atom is inside the cavity the problem is well described by the Jaynes- Cummings Hamiltonian (J-C) [12] only and when the atom exits the cavity the coupling between the heat bath and the single mode is switched on.

In this work a different approach to this problem is introduced. in general at any point in time of the motion we solve for the total density operator ρ for the atom plus the field, that is, the coupling between the cavity field and the heat bath is switched on throughout the whole motion and not only when the cavity is empty of atoms. The damping process is governed by the master equation of the damped harmonic oscillator given by equation [13]

$$\mathcal{L}\rho(t_i) \equiv -\kappa(n_{th} + 1)[a^\dagger a \rho + \rho a^\dagger a + a \rho a^\dagger] - \kappa n_{th}[a a^\dagger \rho + \rho a a^\dagger + a \rho a^\dagger] \quad (1)$$

(1) We illustrate the case when atoms enter the cavity in a coherent superposition state.

We use the J-C model as a fundamental model where the total Hamiltonian of the system (atom + field) is given by [12]

$$H = \hbar\omega a^\dagger a + \hbar\omega_0 \sigma_z + \hbar g(a^\dagger \sigma_- + a \sigma_+) \quad (2)$$

For the case of the single cavity mode is coupled to the heat bath at temperature $T > 0$, and the atom is coupled to this bath only via this cavity mode, the total density operator ρ for atom plus field satisfies the master equation for the high Q-cavity which is given by

$$\dot{\rho}(t) = -i[H, \rho] - \kappa(n_{th} + 1)[a^\dagger a \rho(t) - 2 a \rho(t) a^\dagger + \rho(t) a^\dagger a] - \kappa n_{th}[a a^\dagger \rho(t) - 2 a^\dagger \rho(t) a + \rho(t) a a^\dagger] \quad (3)$$

Where H is the J-C Hamiltonian eqn.(2) when and only when there is a single atom in the cavity. On the other hand when there is no atom in the cavity the above differential equation becomes:

$$\dot{\rho}(t) = -i[H_0, \rho] - \kappa(n_{th} + 1)[a^\dagger a \rho(t) - 2 a \rho(t) a^\dagger + \rho(t) a^\dagger a] - \kappa n_{th}[a a^\dagger \rho(t) - 2 a^\dagger \rho(t) a + \rho(t) a a^\dagger] \quad (4)$$

Where $H_0 = \hbar\omega a^\dagger a$ is the Hamiltonian of the cavity field, $\kappa = \frac{1}{2} \omega Q^{-1}$ is the cavity damping constant with Q is the cavity quality factor. The cavity damping time is $T_c = (2\kappa)^{-1}$

Since the two-level atom is in a coherent state i.e.

$$|\psi\rangle = \alpha |e\rangle + \beta |g\rangle \quad (5)$$

$$\text{with } |\alpha|^2 + |\beta|^2 = 1$$

Since the coupling between the atom with upper state $|e\rangle$ and lower state $|g\rangle$ and the single mode radiation field is present during the motion the space is spanned by states $|g\rangle |0\rangle, |e\rangle |n\rangle, |g\rangle |n+1\rangle$ for $n=0,1,2,\dots$ here $|0\rangle$ is a vacuum state. In this case we should solve for the four coupled elements: $\rho_{e,n}; e, m, \rho_{g,n+1}; g, m+1, \rho_{e,n}; g, m+1, \rho_{g,n+1}; e, m$

The differential equations for these coupled elements can be written in matrix form as:

$$\dot{\psi}^{(k)}(n, t) = \bar{A}^{(k)}(n) \psi^{(k)}(n, t) + B^{(k)}(n) \psi^{(k)}(n+1, t) + C^{(k)}(n) \psi^{(k)}(n-1, t) \quad (6)$$

In which the $\psi^{(k)} \equiv \psi(n, m)$ and $k = m - n$ represents the degree of off-diagonality

The 4-column vectors $\psi^{(k)}(n, t)$ are

$$\psi^{(k)}(n, t) = \begin{pmatrix} \rho_{e,n-1;e,m-1}(t) \\ \rho_{g,n;g,m}(t) \\ \rho_{e,n-1;g,m}(t) \\ \rho_{g,n;e,m-1}(t) \end{pmatrix} \quad (7)$$

And the 4×4 matrices $\bar{A}^{(k)}(n)$, $B^{(k)}(n)$, $C^{(k)}(n)$ are

$$\bar{A}^{(k)}(n) \equiv A(n, m) = \begin{pmatrix} F_a(n+m+1) & 0 & ig\sqrt{m} & -ig\sqrt{n} \\ 0 & F_a(n+m+1) & -ig\sqrt{n} & ig\sqrt{m} \\ ig\sqrt{m} & -ig\sqrt{n} & i\Delta + F_a(n+m) & 0 \\ -ig\sqrt{n} & ig\sqrt{m} & 0 & i\Delta + F_a(n+m) \end{pmatrix} \quad (8)$$

$$B^{(k)}(n) \equiv B(n, m) = \begin{pmatrix} F_b(n, m) & 0 & 0 & 0 \\ 0 & F_b(n+1, m+1) & 0 & 0 \\ 0 & 0 & F_b(n, m+1) & 0 \\ 0 & 0 & 0 & F_b(n+1, m) \end{pmatrix} \quad (9)$$

$$C^{(k)}(n) \equiv C(n, m) = \begin{pmatrix} F_c(n-1, m-1) & 0 & 0 & 0 \\ 0 & F_b(n, m) & 0 & 0 \\ 0 & 0 & F_b(n-1, m) & 0 \\ 0 & 0 & 0 & F_b(n, m-1) \end{pmatrix} \quad (10)$$

With,

$$\begin{aligned} F_a(n+m) &= -2\kappa n_{th}[(n+m) + (n+m-1)] \\ F_b(n, m) &= 2\kappa(n_{th}+1)\sqrt{nm} \\ F_c(n, m) &= 2\kappa n_{th}\sqrt{nm} \end{aligned} \quad (11)$$

Exact Solution:

Now we solve the equations of motion of the density matrix ρ which are expressed in the matrix form eqn.(6).

First of all we assume that all atoms are prepared in the coherent superposition of their upper and lower states namely

$$\rho_{atom} = |\psi\rangle\langle\psi|$$

$$\rho_{atom} = |\alpha|^2 \rho_{e,e} + \alpha^* \beta \rho_{g,e} + \alpha \beta^* \rho_{e,g} + |\beta|^2 \rho_{g,g} \quad (12)$$

Where eqn.(5) has been used

The single mode cavity radiation field is initially in a diagonal thermal state $(nth)^n \rho_{n,m} = \delta_{n,m} (\text{-----}nth+1)n+1$

(13) Where n_{th} is the thermal photons inside the cavity.

For $n=0, m=0$ from eqn.(7) we put

$$\psi^{(0)}(0, t) = \begin{pmatrix} 0 \\ \rho_{g,0;g,0}(t) \\ 0 \\ 0 \end{pmatrix} \quad (14)$$

At $t=0$ and for $(n=0, m=0)$

$$\psi^{(0)}(0,0) = \begin{pmatrix} 0 \\ |\beta|^2 \frac{1}{(n_{th}+1)} \\ 0 \\ 0 \end{pmatrix} \quad (15)$$

And for $(n>0, m>0)$,

$$\psi^{(k)}(n, 0) = \begin{pmatrix} |\alpha|^2 \frac{(n_{th})^{n-1}}{(n_{th}+1)^n} \\ |\beta|^2 \frac{(n_{th})^n}{(n_{th}+1)^{n+1}} \\ 0 \\ 0 \end{pmatrix} \quad (16)$$

In order to solve eq. (6) with the initial conditions eqns. (12-16) we take the Laplace transformation

$\psi^{(k)}(n, z)$ of $\psi^{(k)}(n, t)$ namely

$$\bar{\psi}^{(k)}(n, z) = \int_0^\infty \exp(-zt) \psi^{(k)}(n, t) dt \quad (17)$$

From eq. (6) this transformation gives the following three-term matrix recurrence relations,

$$A^{(k)}(n)\bar{\psi}^{(k)}(n, z) + B^{(k)}(n)\bar{\psi}^{(k)}(n+1, z) + C^{(k)}(n)\bar{\psi}^{(k)}(n-1, z) = -\psi^{(k)}(n, 0) \quad (18)$$

Where $A^{(k)}(n) = \bar{A}^{(k)}(n) - zI$, (I is an identity matrix)

Apparently this equation (18) is a three-term matrix recurrence relation in terms of n and since it is also a three-term matrix recurrence relations in terms of m it is sufficient to work with labels n only for fixed k (n and $n+k$) Following Risken [14] these three-term matrix recurrence relations eqns.(18) have solutions expressible in terms of matrix continued fractions. To get the solution one can truncate these equations at the (N th, M th) term. Thus

$$\bar{\psi}^{(k)}(n) = 0, \quad \forall n > N, \quad \text{and } m > M \quad (19)$$

By inserting the ansatz

$$\bar{\psi}^{(k)}(n, z) = \bar{S}^{+(k)}(n-1, z)\bar{\psi}^{(k)}(n-1, z) + \bar{a}^{(k)}(n, z) \text{.for } n \geq 0, \text{ and /or } \kappa \geq -n \quad (20)$$

in the eqn.(18) yields

$$\begin{aligned} A^{(k)}(n)[\bar{S}^{+(k)}(n-1)\bar{\psi}^{(k)}(n-1) + \bar{a}^{(k)}(n)] + B^{(k)}(n)[\bar{S}^{+(k)}(n)\bar{\psi}^{(k)}(n) + \bar{a}^{(k)}(n+1)] \\ + C^{(k)}(n)[\bar{S}^{+(k)}(n-2)\bar{\psi}^{(k)}(n-2) + \bar{a}^{(k)}(n-1)] \\ = -\psi^{(k)}(n, 0) \end{aligned} \quad (21)$$

It should be understood that the functions $\bar{S}^{+(k)}$, $\bar{\psi}^{(k)}$, and $\bar{a}^{(k)}$ are z -dependent.

Now we make truncation to these equations at suitable values of N and M and then by downward iteration we get,

1- For $n=N+1$ and/or $k=M-N+1$

$$\bar{\psi}^{(k)}(n) = 0$$

$$\bar{a}^{(k)}(n) = -\bar{S}^{+(k)}(n-1)\bar{\psi}^{(k)}(n-1) \quad (22)$$

2- For $n=N$ and/or $k=M-N$

$$\bar{S}^{+(k)}(n-1) = (-A^{(k)}(n))^{-1}C^{(k)}(n)$$

$$\bar{a}^{(k)}(n) = (-A^{(k)}(n))^{-1}\bar{\psi}^{(k)}(n, 0) \quad (23)$$

3- For $0 \leq n \leq N-2$ and/or $0 \leq k \leq M-N-2$

$$\bar{S}^{+(k)}(n) = [-A^{(k)}(n+1) - B^{(k)}(n+1)\bar{S}^{+(k)}(n+1)]^{-1}C^{(k)}(n+1) \quad (24)$$

4- For $0 \leq n \leq N-1$ and/or $0 \leq k \leq M-N-1$

$$\bar{a}^{(k)}(n) = [-A^{(k)}(n) - B^{(k)}(n)\bar{S}^{+(k)}(n)]^{-1}[\bar{\psi}^{(k)}(n, 0) + B^{(k)}(n)\bar{a}^{(k)}(n+1)] \quad (25)$$

The solution when the cavity is empty of atoms can be obtained by employing the master equation of the damped harmonic oscillator in the rotating frame that is [13]

$$\dot{\rho}(t) = -\kappa(n_{th} + 1)[a^\dagger a \rho(t) - 2a \rho(t) a^\dagger + \rho(t) a^\dagger a] - \kappa n_{th}[a a^\dagger \rho(t) - 2a^\dagger \rho(t) a + \rho(t) a a^\dagger] \quad (26)$$

where the density matrix ρ is for the micromaser cavity field only. In photon number basis the density matrix elements of this equation are,

$$\begin{aligned} \dot{\rho}^{(k)}(n, t) = 2\kappa(n_{th} + 1) \left[\sqrt{(n+1)(n+k+1)} \rho^{(k)}(n+1, t) + \left(n + \frac{k}{2}\right) \rho^{(k)}(n, t) \right] + \\ 2\kappa n_{th} \left[\sqrt{(n)(n+k)} \rho^{(k)}(n-1, t) - \left(n + 1 + \frac{k}{2}\right) \rho^{(k)}(n, t) \right] \end{aligned} \quad (27)$$

The solution to this differential equation is given by [15]

$$\rho^{(k)}(n, t) = \exp(-\kappa kt) \sum_{i=0}^n \sum_{j=n-i}^\infty C_{n,j,i}^{(k)} \frac{A^j}{B^{j+k+1}} \left(\frac{A}{A}\right)^{n-i} \left(\frac{B}{B}\right)^i \rho^{(k)}(n, 0) \quad (28)$$

where

$$C_{n,j,i}^{(k)} = (-1)^i \binom{i+j+k}{i} \binom{j}{n-i} \left(\frac{j+k}{j}\right)^{\frac{1}{2}} \binom{j+k}{n} \quad (29)$$

$$A = (n_{th} + 1)(1 - \exp(-2\kappa t)) \quad (30)$$

$$B = 1 + n_{th}(1 - \exp(-2\kappa t)) \quad (31)$$

$$A' = \exp(-2\kappa t) - n_{th}(1 - \exp(-2\kappa t)) \quad (32)$$

$$B' = -n_{th}(1 - \exp(-2\kappa t)) \quad (33)$$

Therefore through these relations with suitable values of n and m and by iteration the function

$\bar{\psi}^{(k)}(n, z)$ is delivered and then by the inverse Laplace transformation $\psi^{(k)}(n, t)$ is obtained. After obtaining all $\psi^{(k)}(n, t)$'s ($n=0,1,2,\dots$) we calculate the reduced density matrix elements of the cavity field by tracing over the atomic variables by using the relation

$$\rho_f^{(k)}(n) = Tr_{atom} \rho^{(k)}(n) \quad (34)$$

The diagonal elements of the density matrix $\rho(0)(n)$ can be used for the calculation of the following physical observables.

1- The average photon number of the micromaser field

$$\langle n \rangle = Tr(n\rho^{(0)}(n)) \quad (35)$$

2- The normalized variance in the photon number

$$v = \sqrt{\frac{\langle n^2 \rangle - \langle n \rangle^2}{\langle n \rangle}} \quad (36)$$

3- The entropy of the micromaser field

$$S = -Tr[\rho \ln(\rho)]$$

$$S = -\sum_{n=0}^{\infty} \rho_{nn} \ln \rho_{nn} \quad (37)$$

This equation is for the case when ρ is diagonal that is when $|\alpha|^2 = 1$ only When $|\alpha|^2 \neq 1$ the density matrix becomes ρ_{nm} instead of ρ_{nn} namely

$$S = -\sum_{n,m} \rho_{nm} \ln \rho_{nm} \quad (38)$$

Numerical results and Calculations

In these calculations the investigations will be for case when the atoms are in their upper states where $|\alpha| = 1$ and $|\beta| = 0$. For $Q = 5 \times 10^{10}$, $gt_{int} = 1.54$, $gT_p = 308$ and $T = 0.5 K$ With regular inputs, the cavity field evolves towards a steady state as in Fig.(1a). Initially the trapping state at

$n=3$. For $gt_{int} = \frac{\pi}{2}$ appears to play a significant rule because P_3 rises to $P_3 = 0.69$ for $N=25$ Fig.(1e) but since $gt_{int} < \frac{\pi}{2}$, $n=3$ is not an exact trapping state. However it is $n=13$ and not $n=15$ (the 2nd trapping state) which plays an important role even for $N=50$ ($P_{13}=0.043$). Similarly for $N=150$ ($P_{13}=0.15$). Ultimately, the cavity field reaches a steady state and the $P_{13}=0.322$ is the largest P_n in a bell-shaped grouping in $11 \leq n \leq 16$ centred about it as $N=1000$. The average photon number $\langle n \rangle$ Fig.(1a) rises rapidly from black body value to nearly $n=3$ (the first trapping state), then jumps this state and steadily increased towards the second trapping state $n=15$, and since $gt_{int}=1.54$ the field traps at $n \approx 13$ ($n=13.387$ at $N=1000$) for the reasons mentioned above.

The variance Fig. (1b) initially drops from black-body value to $v=0.35$ at $N=7$ then increases to its most maximum $v=1.94$ at $N=98$ where it starts decreasing towards a nearly steady value $v=0.384$ at $N=1000$ The entropy S Fig.(1c) shows that the cavity field ultimately evolves towards a mixed state. Similarly the probability $P|e\rangle$ that the atom exits the cavity in its upper state initially increases Fig. (1d) and becomes large compared with $P|g\rangle$ that is the probability of lower state, then it decreases slowly and finally reaches a fixed value.

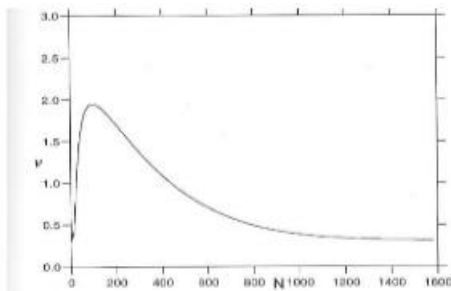


Figure 1(b) The variance of the cavity field as a function of the number of atoms N , for the case of regular inputs, the parameters are those of Fig.(a).

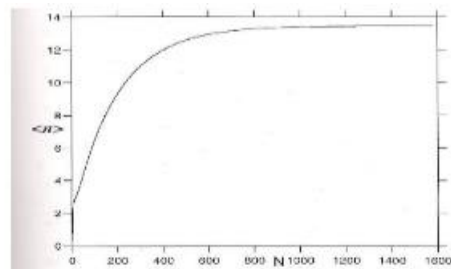


Figure 1(a) The average photon number in the cavity field as a function of the number of atoms N , for the case of regular inputs, $|\alpha| = 1$, $Q = 5 \times 10^{10}$, $gt_{int} = 1.54$, $gT_p = 308$ and the initial average thermal photon number in the cavity is $n_{th} = 0.13$.

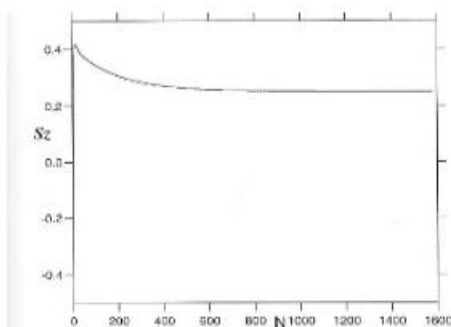


Figure 1(d) The atomic population difference as a function of the number of atoms N , for the case of regular inputs, the parameters are those of Fig.(a)

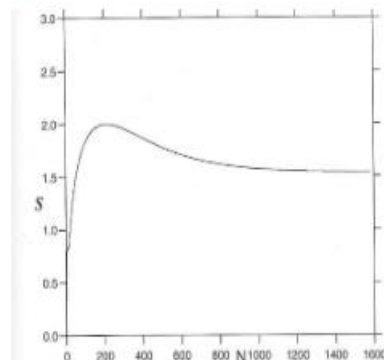


Figure 1(c) The entropy S as a function of the number of atoms N , for the case of regular inputs, the parameters are those of Fig.(a).

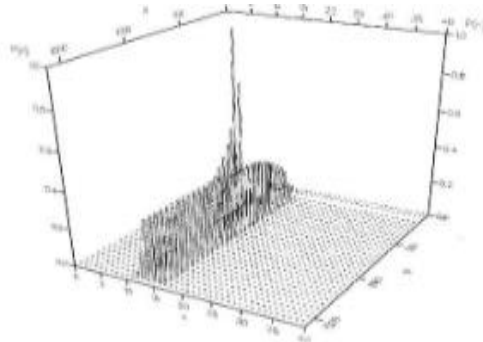


Figure (1 c) The photon number distribution P_n vs n (the photon number) and N (the number of atoms) for the case of regular inputs, the parameters are those of Fig.(a).

The effect of the cavity temperature T on the micromaser field is shown in Figures (2). For $T=70\text{mK}$ with fixed parameters as in Figures (1), the micromaser field evolves towards a steady state similar to the situation of Figs.(1), namely the change in the micromaser field is a quantitative change and not a qualitative change when the temperature of the cavity is reduced to this very low value and the other parameters are kept constant (fixed). The main difference between the observations of Figs. (1) And Figs.(2) is that: a long time (large number of atoms) is needed before reaching a steady state when the temperature of the cavity becomes very low. This is clear when we realize that the steady state is nearly reached in Fig.(1) when approximately 103 atoms have passed through the cavity, where as in Fig.(2), up to 2800 atoms, the field is still in its way to a steady state and it does not reach it yet .

In addition to the effects of the temperature in this regime we also investigate (through figures3) the effects of the cavity

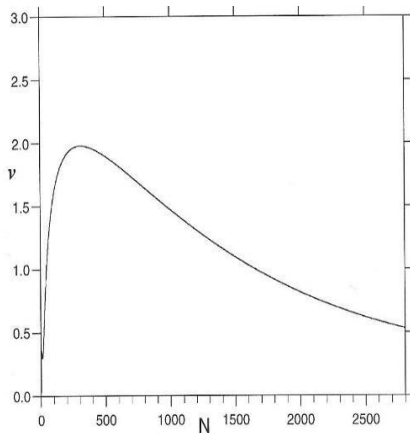
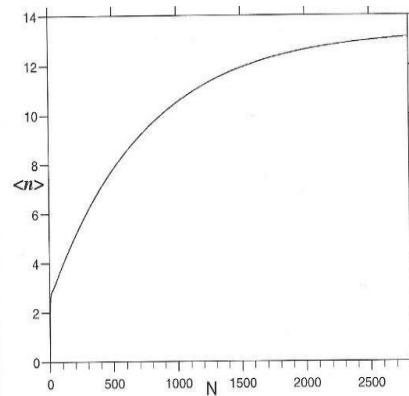


Figure (2b) The variance of the cavity field as a function of the number of atoms N , for the case of regular inputs, the parameters are those of Fig.(a).



Figure(2a) The average photon number in the cavity field as a function of the number of atoms N , for the case of regular inputs, $|\alpha| = 1$, $Q = 5 \times 10^{10}$, $g_{int}^2 = 1.54$, $gT_p = 308$ and the initial average thermal photon number in the cavity is $n_{th} = 10^{-7}$.

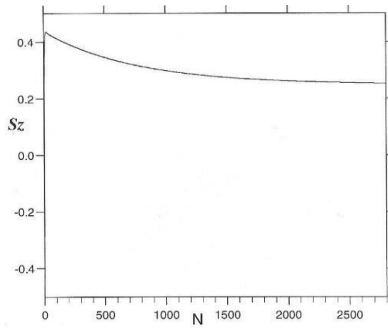


Figure (2d) The atomic population difference as a function of the number of atoms N , for the case of regular inputs, the parameters are those of Fig.(a).

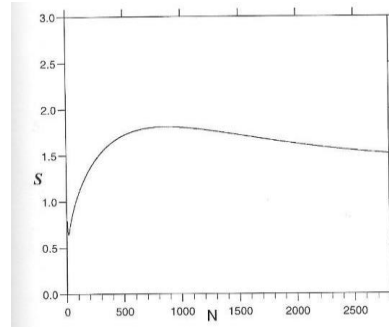


Figure (2c) The entropy S as a function of the number of atoms N , for the case of regular inputs, the parameters are those of Fig.(a).

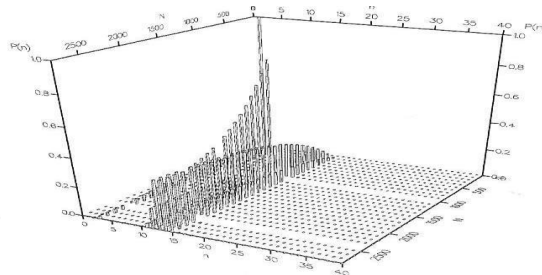
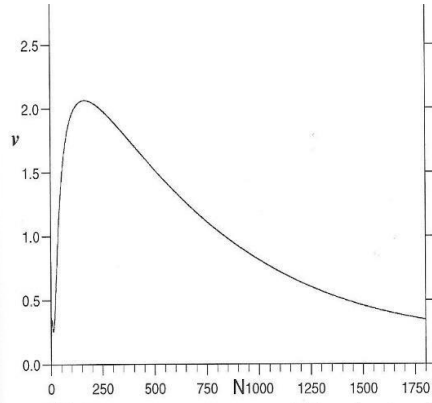


Figure (2e) The photon number distribution P_n vs n (the photon number) and N (the number of atoms) for the case of regular inputs, the parameters are those of Fig.(a).

For the parameters of Fig.(2) but $Q = 19 \times 10^{10}$, we plot in Figs.(3) the same observables as in Figs.(2). We find that the average photon number $\langle n \rangle$ behaves initially similar to that of Fig.(1a) and Fig.(2a), but as N increases the photon number evolves towards a steady state and traps at $N=15$ (Fig.(3a),Fig.(3e)) instead of $N=13$ as in the previous figures. It is evident that the increase in Q value enhances the quantum character of the cavity field such as the sub-Poisson statistics (Fig.3b), namely the quantum features become apparent more and more by increasing the cavity quality factor Q . Moreover the purity of the cavity field is improved by increasing Q even though the evolution is still towards a mixed state as before. The difference between $P_{|e\rangle}$ and $P_{|g\rangle}$ is nearly fixed at large N (Fig.(3d)).



Figure(3b) The variance of the cavity field as a function of the number of atoms N , for the case of regular inputs, the parameters are those of Fig.(a).

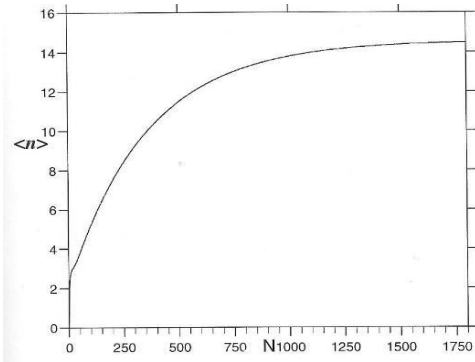
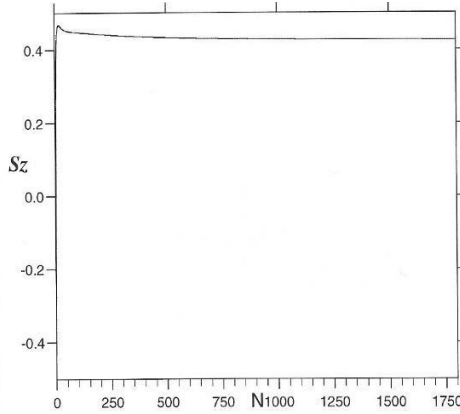
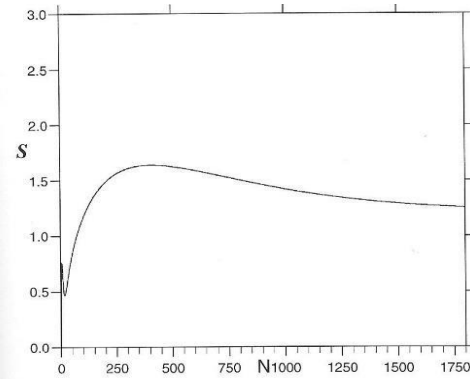


Figure (3a) The average photon number in the cavity field as a function of the number of atoms N , for the case of regular inputs, $|\alpha| = 1$, $Q = 19 \times 10^{10}$, $gt_{int} = 1.54$, $gT_p = 308$ and the initial average thermal photon number in the cavity is $n_{th} = 10^{-7}$.



Figure(3d) The atomic population difference as a function of the number of atoms N , for the case of regular inputs, the parameters are those of Fig.(a).



Figure(3c) The entropy S as a function of the number of atoms N , for the case of regular inputs, the parameters are those of Fig.(a).

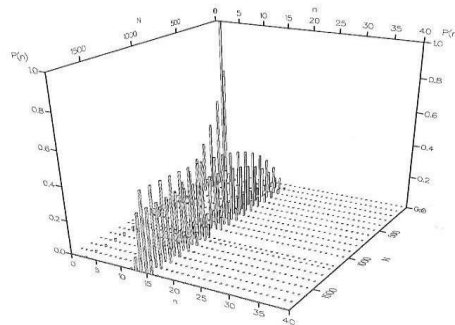
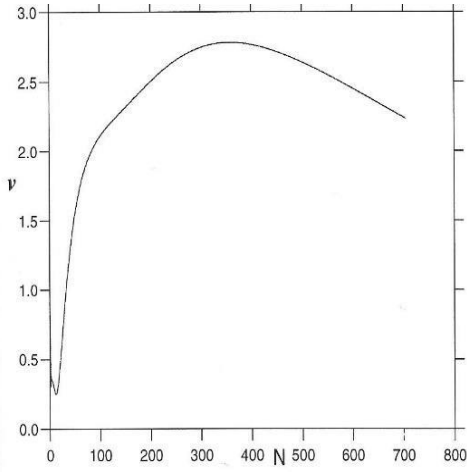


Figure (3e) The photon number distribution P_n vs n (the photon number) and N (the number of atoms) for the case of regular inputs, the parameters are those of Fig.(a).

To achieve a qualitative change in the micromaser we plot in Fig.(4) the same quantities of Fig.(1) but with $gt_{int} \equiv gT_p = 1.54$ and the other parameters are fixed. Even for this high temperature T and for this large value of Q no steady state in the variance ν is apparent for this range of N . Moreover, the dynamics of the cavity field, for this set of parameters, can be described as non-steady trapping state dynamics [] where P_3, P_{16}, P_{36} (Fig.4e) play a significant role in this dynamics. In this situation the average photon number Fig.(4a) continues its increase after passing both, the first trapping state $N=3$ and the second trapping state $N=15$. The variance ν Fig.(4b) falls from black-body value to $\nu=0.249$ at $N=12$ and rises to its maximum $\nu=2.78$ at $N=358$, beginning a slow decrease afterwards. The measure of the state purity S is shown in Fig.(4c).For this range of N , the number of atoms, the cavity field is still evolving towards a mixed state $S>0$ (and still increasing) rather than a pure state (an evolution towards pure state occurs at $4 \leq N \leq 19$ however). The probability $P_{|e\rangle}$ is still larger than $P_{|g\rangle}$ at higher N 's (Fig.(4d)).



Figure(4b) The variance of the cavity field as a function of the number of atoms N , for the case of regular inputs, the parameters are those of Fig.(a).

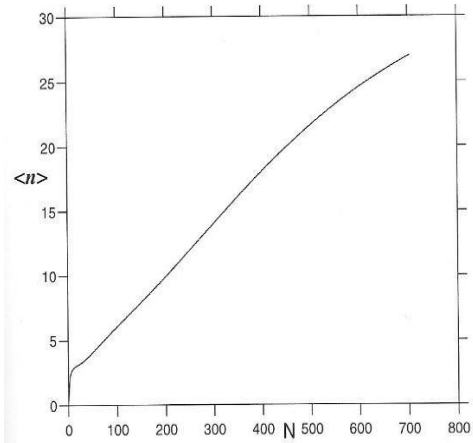
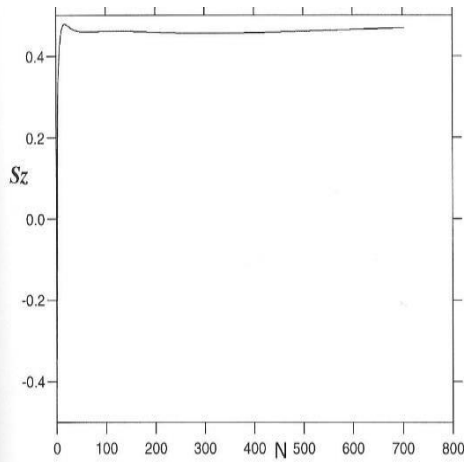


Figure (4a) The average photon number in the cavity field as a function of the number of atoms N , for the case of regular inputs, $|\alpha| = 1$, $Q = 5 \times 10^{10}$, $gt_{int} = 1.54$, $gT_p = 1.54$ and the initial average thermal photon number in the cavity is $n_{th} = 0.15$.



Figure(4d) The atomic population difference as a function of the number of atoms N , for the case of regular inputs, the parameters are those of Fig.(a).

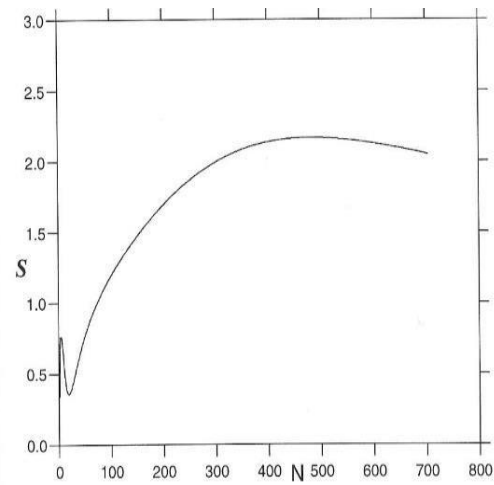
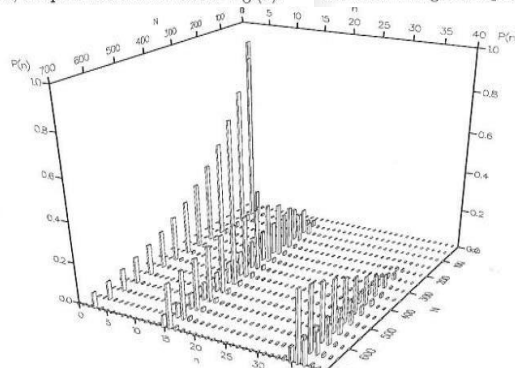
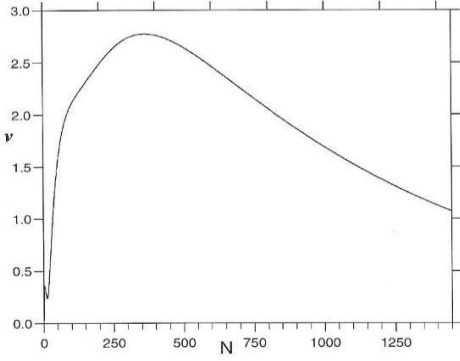


Figure (4c) The entropy S as a function of the number of atoms N , for the case of regular inputs, the parameters are those of Fig.(a).

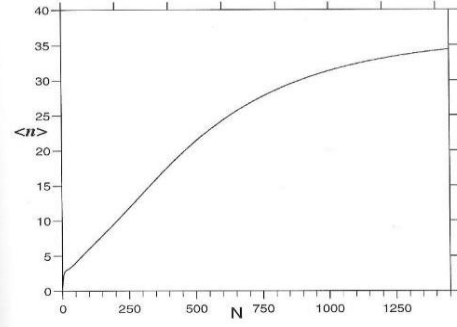


Figure(4e) The photon number distribution P_n vs n (the photon number) and N (the number of atoms) for the case of regular inputs, the parameters are those of Fig.(a).

To investigate the effects of the reduction of the cavity temperature T in this regime, we plot in figures 5 the same quantities for $T=70\text{mK}$ and the other parameters are kept constant as in figures 4. From all the figures it is apparent that the reduction of the cavity temperature has no clear effect on the behaviour of the cavity field in the "trapping state dynamics" regime. Therefore, when the trapping states are effective (trapping state dynamics) the micromaser field becomes insensitive to the changes in T and Q .



Figure(5b) The variance of the cavity field as a function of the number of atoms N , for the case of regular inputs, the parameters are those of Fig.(a).



Figure(5a) The average photon number in the cavity field as a function of the number of atoms N , for the case of regular inputs, $|\alpha| = 1$, $Q = 5 \times 10^{10}$, $gt_{int} = 1.54$, $gT_p = 1.54$ and the initial average thermal photon number in the cavity is $n_{th} = 10^{-7}$.

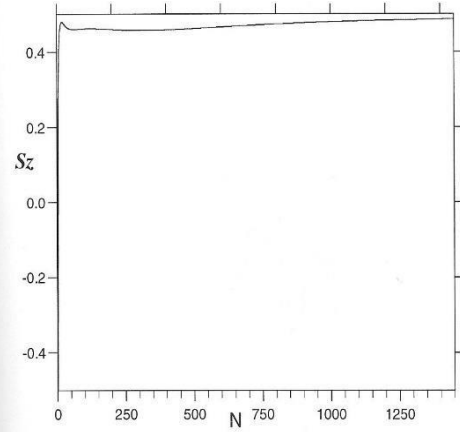
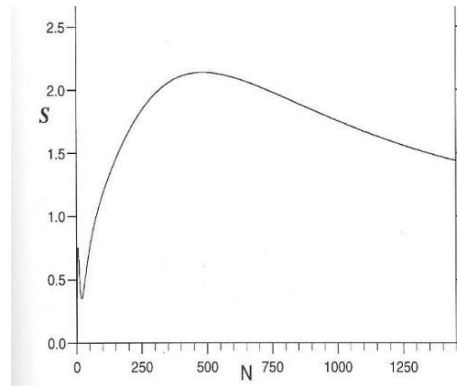


Figure (5d) The atomic population difference as a function of the number of atoms N , for the case of regular inputs, the parameters are those of Fig.(a).



Figure(5c) The entropy S as a function of the number of atoms N , for the case of regular inputs, the parameters are those of Fig.(a).

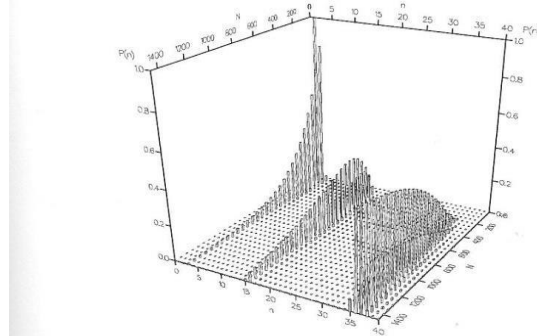


Figure (5e) The photon number distribution P_n vs n (the photon number) and N (the number of atoms) for the case of regular inputs, the parameters are those of Fig.(a).

CONCLUSION

We report a numerical simulation of the action of the one ^{85}Rb atom micromaser which shows that the micromaser field evolves towards a steady state equilibrium when the condition that $T_p \gg t_{int}$ satisfies. In this steady state regime the cavity field reaches a steady state after a sufficient number of atoms have passed through the cavity. The cavity temperature T and the cavity quality factor Q can produce a quantitative change when one of them or the two are changed but they are not responsible for the qualitative changes in the micromaser field. Evidently the only responsible parameter for these qualitative changes is the repetition time T_p namely if $T_p \gg t_{int}$ then the micromaser field evolution is towards a steady state equilibrium. In contrast when T_p reduced to the order of t_{int} then the micromaser field evolution is controlled by the trapping state dynamics – no steady state is apparent in this case.

The first going-up trapping state at $n=3$ plays a significant role in the early dynamics of the micromaser field. Moreover the state of the field ultimately evolves towards a mixed state rather than a pure state. This is happened may be because of three reasons, the first is the presence of the cavity field damping which destroy completely the purity of the field[15], the second reason is that, when a trapping state is present in between a down trapping state and an upper trapping state then the situation becomes complicated [16] (and consequently no evolution towards a pure state). In our situation the presence of the first trapping state at $n=3$ in between the going-down trapping state at $n=0$ and the second trapping state at $n=15$ prevents the field from evolving towards a pure state, and the third reason is that, the presence of the black-body

radiation initially in the cavity destroys coherence induced in the micromaser field. These three unavoidable effects are responsible for destroying the purity of the micromaser field.

REFERENCES

- [1]. P. Filipowicz, J. Javanainen, and P. Meystre, Phys. Rev. A34, (1986), 3077.
- [2]. L. Lugiato, M.O. Scully, and H. Walther, Phys. Rev. A36, (1987), 740.
- [3]. R. K. Bullough, N. Nayak and B. V. Thompson: in "Recent development in quantum Optics" ed. by R. Ingova (Plenum N.Y. 1993).
- [4]. P. Lougovski, F. Casagrande, A. Lulli, B.G. Englert, E. Solano, and H. Walther, Phys. Rev. A 69, 023812 (2004).
- [5]. F. Casagrande, B. G. Englert, P. Lougovski, A. Lulli, E. Solano, and H. Walther, Opt. Spectrosc. 99, (2005), 30
- [6]. D. Yu, L. Chuan Kwek, L. Amico, and R. Dumke Phys. Rev. A95, 53811, (2017).
- [7]. C. Fang Yen, 1, *C. C. Yu, S. Ha, W. Choi, K. An, R. R. Dasari, and M. S. Feld Phys. Rev. A73, 041802 R (2006).
- [8]. A.M. Kremid, AL-NAWAH, 8 (12), (2009), 14-20.
- [9]. D. Meschede, H. Walther and H. Mül semiclassical. Opt. 2 (2000), 154.
- [10]. S. Brattke, G. R. Guthohrlein, M. Keller, W. Lange, B. Varcoe and H. Walther, J. Mod. Optics. 50 (6-7): (2003), 1103-1113.
- [11]. M. Weidinger, B. T. H Varcoe, R. Heerlein and H. Walther, Phys. Rev. Lett, 82, (19), (1999), 3795-3798.
- [12]. E. T. Jaynes and F. W. Cummings, Proc. IEEE, 51, (1963), 89.
- [13]. G .S. Agarwal, in "Springer Tracts in Modern Physics" vol, 70 (Springer Verlag), (1974).
- [14]. H. Risken, 'The Fokker Planck Equations', 1984 (Spriger –Verlage – Berlin).
- [15]. P. Bogar, J. A. Berguo and M. Hillery, Phys. Rev. A51, (1995), 2381.
- [16]. J. J. Slosser, P. Meystre, E. M. Wright, Opt. Lett. 15,(1990), 233.